Results in Engineering 29 (2026) 108456

Contents lists available at ScienceDirect

Results in Engineering

journal homepage: www.sciencedirect.com/journal/results-in-engineering

Real-time BioContact assurance and status monitoring using human body communication

Rajat Kumar [a,*], Abdelhay Ali [a], Abdulkadir Celik [b], Ahmed M. Eltawil [a]

[a] King Abdullah University of Science and Technology (KAUST), Thuwal, 23955, Saudi Arabia
[b] University of Southampton, Southampton, SO17 1BJ, United Kingdom

ARTICLE INFO

Keywords:
Biomedical applications
Electrodes
Human body communication
Internet of bodies

ABSTRACT

Reliable electrode-skin contact is essential for accurate biomedical signal acquisition, as poor contact leads to signal degradation and measurement errors in critical applications such as ECG, EEG, and EMG monitoring. Traditional lead-off detection methods face real-world challenges, including motion artifacts causing false detections, environmental noise reducing accuracy, and variations in skin-electrode impedance affecting reliability. To address these limitations, this paper presents a BioContact assurance system (BCAS) leveraging common-ground human body communication (CG-HBC) to continuously monitor electrode contact status. CG-HBC enables direct digital communication through the human body without complex modulation. The system consists of three core components: a CG-HBC transceiver, a processing unit, and an electrode interface module. The CG-HBC transceiver, fabricated using the TSMC 65 nm process, achieves 11.55 pJ/bit energy efficiency and consumes only 23.10 μW, making it suitable for seamless integration into wearable medical devices. A custom timing protocol synchronized with biomedical sampling ensures consistent and reliable contact monitoring. BCAS accurately classifies electrode conditions (connected, loose, intermittent, disconnected) in real time by analyzing the bit error rate and transmission success rate between electrode pairs, ensuring reliable contact assessment while maintaining signal quality. Unlike traditional DC/AC lead-off techniques, it detects subtle contact degradations with high sensitivity while sustaining robust performance for fully connected or disconnected states. These advancements highlight its promise for next-generation continuous health monitoring systems and intelligent biomedical wearables.

1. Introduction

The concept of the Internet of bodies (IoB) has revolutionized health monitoring by embedding sensors and devices in, on, or near the human body [1]. The IoB leverages the human body as a communication medium, enabling seamless signal transmission across different body regions [2]. Electrodes play a pivotal role within the IoB ecosystem, enabling biomedical signal acquisition and information transfer. They facilitate communication between the human body and medical devices, crucial for health monitoring, diagnostics, and wearable technology advancements [3]. Electrodes are mainly classified as wet and dry, with advancements leading to types such as semi-dry, dry non-contact, and microneedle array electrodes [4]. Wet electrodes use an electrolyte layer to enhance conductivity by hydrating the skin and reducing impedance at the electrode-skin interface [5]. However, using an electrolyte layer requires careful handling, and prolonged use may cause skin irritation or performance issues due to electrolyte drying [4]. In contrast, dry electrodes eliminate the need for an electrolyte layer and rely on material properties for conductivity. While they offer greater convenience and reduced maintenance compared to wet electrodes, they face challenges such as poor skin contact and interference from air or dust [5]. Moreover, the pressure exerted by dry electrodes must strike a balance between effective operation and user comfort [6].

Reliable biomedical signal acquisition depends on the quality of the electrode-skin interface, making lead-off detection essential for ensuring consistent performance. In addition to maintaining signal quality, detecting disconnections conserves power by shutting down modules and alerts users in a timely manner to improve connections. Traditional methods primarily fall into two categories: DC and AC [7–11]. DC detection measures electrode input voltages relative to supply rails using bias resistors that establish reference thresholds, signaling disconnection when voltage levels approach the rails. It offers simplicity and low power consumption, making it attractive for compact, battery-powered systems. AC lead-off detection, on the other hand, injects high-frequency test signals between electrodes to evaluate impedance changes associated with connectivity status. Despite their advantages, both DC and

* Corresponding author.
E-mail address: rajat.kumar@kaust.edu.sa (R. Kumar).

https://doi.org/10.1016/j.rineng.2025.108456
Received 6 September 2025; Received in revised form 3 November 2025; Accepted 26 November 2025
Available online 6 December 2025

AC techniques exhibit notable limitations. The reliance on threshold-based criteria quantizes the connection state into binary outcomes, connected or disconnected, making it difficult to recognize intermediate or partially detached conditions. Under marginal contact situations, the measured status may fluctuate, leading to unstable detection. In DC-based methods, external pull-up resistors or current sources are required, which add additional noise and cause baseline shifts. Although AC-based methods can capture impedance characteristics, they increase system complexity due to the need for signal demodulation and filtering of superimposed waveforms. These challenges are particularly significant in wearable applications, where constant movement and varying electrode placement affect the skin-electrode interface [12]. In such scenarios, the contact between the electrode and the skin may fluctuate, resulting in brief interruptions in signal transmission [13]. Both methods struggle with real-world challenges: motion artifacts can trigger false detections, environmental noise can reduce accuracy, and varying skin-electrode impedance can compromise reliability.

Recent studies have investigated advanced methodologies such as impedance spectroscopy, embedded neural networks, and passive contact monitoring to enhance lead-off detection reliability. These approaches are designed to improve detection sensitivity, minimize power consumption, and enable real-time evaluation of electrode-skin adhesion under dynamic conditions. Passive monitoring techniques have been introduced to provide basic contact quality assessment; however, their implementation necessitates the integration of additional system components, thereby increasing design complexity and reducing practical feasibility [14]. Neural network-based frameworks have demonstrated accuracies of approximately 98 % in distinguishing between proper adhesion and partial detachment. Nonetheless, implementing such algorithms on microcontrollers requires an average inference time of 4.286 ms, which may constrain their applicability in biomedical platforms [15]. While these emerging techniques exhibit significant potential, they are not yet suitable for all biomedical applications due to implementation complexity and processing demands. Consequently, addressing variations in biointerface impedance, minimizing motion-induced artifacts, and establishing standardized evaluation protocols for consistent performance remain major challenges.

To address these challenges, this article proposes a new BioContact assurance system (BCAS) leveraging common-ground human body communication (CG-HBC) technology to ensure reliable real-time electrode contact. CG-HBC utilizes the conductive properties of human tissue as a transmission medium for digital signals. The proposed system transmits digital data packets between electrodes through the human body and analyzes reception quality, transmission success rates, and signal integrity to determine electrode connectivity status. Extensive research on implantable and wearable intrabody communication demonstrates that electrode configuration and coupling mode play a critical role in determining propagation characteristics and channel attenuation, thereby influencing bit error rate (BER) and signal reliability [16]. Consequently, detailed channel characterization becomes crucial to understanding how signal propagation is affected by tissue composition, electrode placement, and the surrounding environment. Such characterization enables the development of accurate propagation models that account for frequency-dependent attenuation, coupling impedance, and parasitic interactions, which are essential for optimizing transmission reliability and minimizing energy loss in body area networks [17–19]. Since the ground reference is shared within BCAS under the CG-HBC topology, the implementation and optimization are simplified due to reduced circuit complexity compared with galvanic or capacitive coupling. The system continuously monitors electrode contact, detecting contact loss or signal fluctuations. It introduces several key advancements:

1. The system employs direct digital communication between electrodes through the human body, providing enhanced robustness and reliability compared to conventional impedance-based detection techniques.
2. An optimized time-slotted transmission protocol is implemented to accommodate the diverse sampling requirements of various biomedical applications.
3. A custom-designed integrated circuit architecture for CG-HBC transceiver (TRx) achieves ultra-low power consumption, ensuring extended battery life and sustainable performance in resource-constrained wearable healthcare applications.

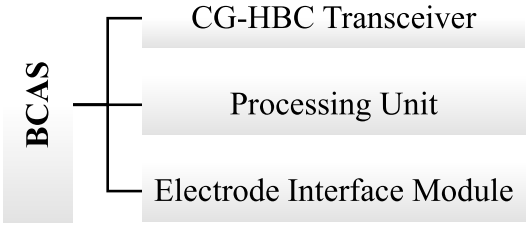

Fig. 1. Functional block diagram of the proposed BCAS system.

These features not only improve signal acquisition reliability but also enable timely intervention in the case of suboptimal electrode performance, ensuring continuous and precise clinical measurements. Compared to traditional lead-off detection methods, the proposed system offers several advantages. By eliminating the need for external resistors or current sources, it reduces noise and baseline shifts. It enhances reliability by detecting individual electrode disconnections and is compatible with systems featuring various electrode configurations, which is crucial for multichannel systems. Furthermore, it seamlessly integrates with existing devices without requiring hardware modifications, utilizing existing processing units for efficient operation. These features collectively reduce system complexity, and the system's effectiveness in detecting false or loose connections makes it suitable for applications such as wearable biomedical monitoring, long-term physiological data acquisition, and implantable sensing systems, where reliable electrode contact is critical for maintaining signal integrity and ensuring patient safety.

The main contributions and innovations of this work are summarized as follows:

1. A new BCAS architecture is proposed to ensure reliable and real-time electrode contact monitoring.
2. A compact CG-HBC TRx chip is designed and fabricated, featuring low-power operation.
3. A complete system prototype is developed by integrating the proposed architectures, and its capability to accurately detect the contact states of an electrode pair is experimentally validated.
4. A comprehensive comparison with conventional AC/DC detection approaches is conducted, demonstrating the superior performance of the proposed system.

2. BioContact assurance system

The BCAS validates electrode contact by transmitting predefined digital patterns across electrode pairs and evaluating transmission success, error characteristics, and signal integrity to assess connectivity. The proposed system, illustrated in Fig. 1, consists of three primary components: (1) a CG-HBC TRx, which forms the core of the system and represents the key novel component added to existing biomedical measurement systems; (2) a processing unit to perform necessary calculations for electrode status detection, which could either utilize the processing capabilities of existing measurement systems or function as a standalone

microcontroller (MCU); and (3) an electrode interface module to manage electrode connections in multi-electrode setups, required only for systems with more than two electrodes such as multi-lead ECG configurations.

Several approaches have been developed to implement human body communication (HBC): i) capacitive coupling uses the body as a forward path and environmental coupling as a return path; ii) galvanic coupling employs differential signal transmission through body tissue; and iii) magnetic coupling utilizes magnetic fields induced in the body [1]. For electrode contact monitoring, where the primary goal is reliable and continuous verification of electrode connectivity, we introduce a simplified CG-HBC approach where transmitter (Tx) and receiver (Rx) share a common ground on the same device. This eliminates complex analog front-end circuitry typically required in conventional HBC Rxs, enabling pure digital transmission while reducing system complexity, lowering power consumption, and enhancing signal reliability by minimizing degradation and interference commonly observed in other HBC implementations.

2.1. System architecture

The overall BCAS architecture for N electrodes is shown in Fig. 2, representing one possible implementation of the proposed concept that employs a CG-HBC TRx, a standalone processing unit, and an electrode interface module for validation purposes. This exemplary system includes an OLED display for electrode status indication and an MCU serving as the processing unit. The modular design allows for versatile implementation approaches: the system can be seamlessly integrated into existing monitoring equipment with minimal hardware additions (primarily the CG-HBC TRx component), or deployed as a comprehensive standalone solution as depicted in the figure. At the core of this framework is the CG-HBC TRx, which integrates essential functionalities for signal processing, control, and communication. It communicates with a compact processing unit through a universal asynchronous receiver-transmitter (UART) interface, where the MCU serves as a programmable interface, enabling configuration for specific applications such as electrocardiogram (ECG), electroencephalogram (EEG), and electromyogram (EMG). A critical component is the high-pass filter (HPF), which attenuates low-frequency components to remove interference in the frequency range of biomedical signals. This ensures signal accuracy by preventing spectral overlap between measurement and testing signals, thereby enhancing overall performance. The electrode interface module is critical for selecting Tx and Rx electrodes from the available electrodes within the system during measurements. It comprises components such as multiplexers, demultiplexers, encoders, decoders, and finite state machines controlled by a central controller to govern electrode selection. This selection process may follow sequential, time slot-based, or alternative patterns, enabling comprehensive verification of contact status across all electrodes.

The CG-HBC TRx facilitates broadband communication for direct digital data transmission, eliminating the need for complex modulation schemes, as illustrated in Fig. 2. The system supports configurable data rates from 1 kbps to 13.5 Mbps by adjusting the operating clock frequency. Lower data rates minimize power consumption for long-term monitoring and improve signal reliability under suboptimal contact conditions, while higher rates enable rapid electrode status verification for time-critical medical procedures requiring instant feedback, all without interfering with measurement signals. Data transmission begins with incoming data temporarily stored in a FIFO buffer, interfacing with the UART module to ensure reliable handling. The data is then passed to the raw baseband Tx (RBT) for direct transmission through the human body. A programmable clock divider generates the required data rates from the reference clock, ensuring synchronization and operational accuracy. The Tx constructs packets with eight start bits, an 8-bit payload, two stop bits, and a 4-bit break period, forming a robust framing structure for reliable detection. The Rx employs a frame synchronization module featuring a shift register with pattern-matching logic to detect packet boundaries, using start bits to initiate data capture and stop bits with inter-frame gaps to maintain synchronization. A state machine tracks packet structure, ensuring robust recovery even under noise or signal degradation. After synchronization, received data is routed to the UART module through raw baseband Rx (RBR) for further processing. The control logic, managed by a finite state machine, coordinates system operations, including timing and Rx synchronization, while configuration registers allow runtime selection of data rates and modes.

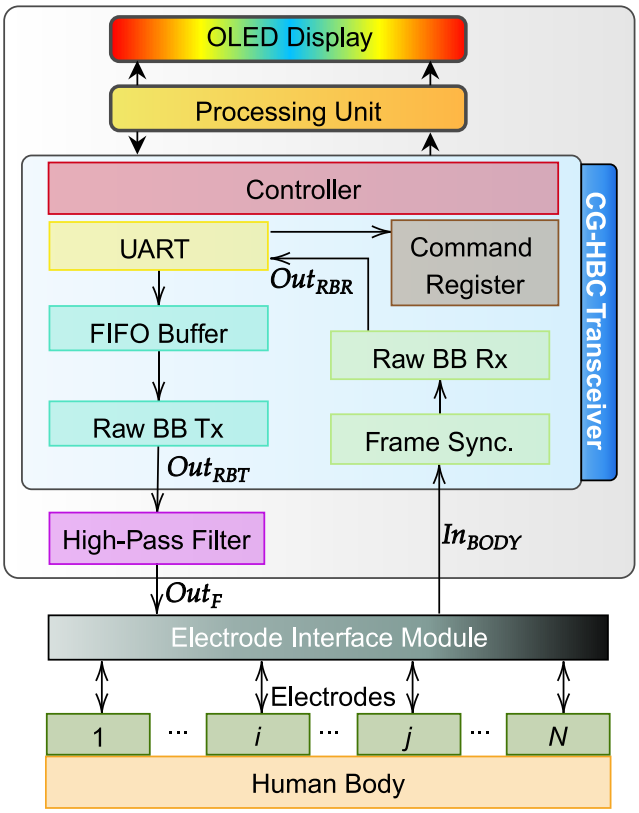

Fig. 2. Block diagram of the BCAS design showing the overall system architecture for N electrodes.

2.2. Transmission protocol for link status detection

To determine the connectivity status of N electrodes, we utilize a time-slotted transmission protocol shown in Fig. 3, where $M_{i,j}$ packets are transmitted to identify the link status between electrodes i and j, $i \neq j, \{i, j\} \in [1, N]$. The packet duration $\Delta = P/R$ depends on packet size, P, and the data rate, R. For a packet size of 8, three data rates – 100 kbps, 1 Mbps, and 2 Mbps – are used in the protocol, resulting in packet durations of 220 μs, 22 μs, and 11 μs, respectively. These data rates are selected considering ECG as the reference application, balancing contact verification time and sampling requirements. Standard ECG sampling rates range from 250 Hz to 1 kHz, with sampling intervals of 1–4 ms. The selected packet durations are significantly shorter than ECG

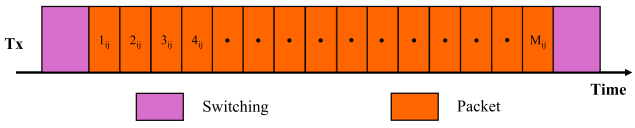

Fig. 3. Pictorial representation of the timing protocol illustrating the time-slotted transmission approach.

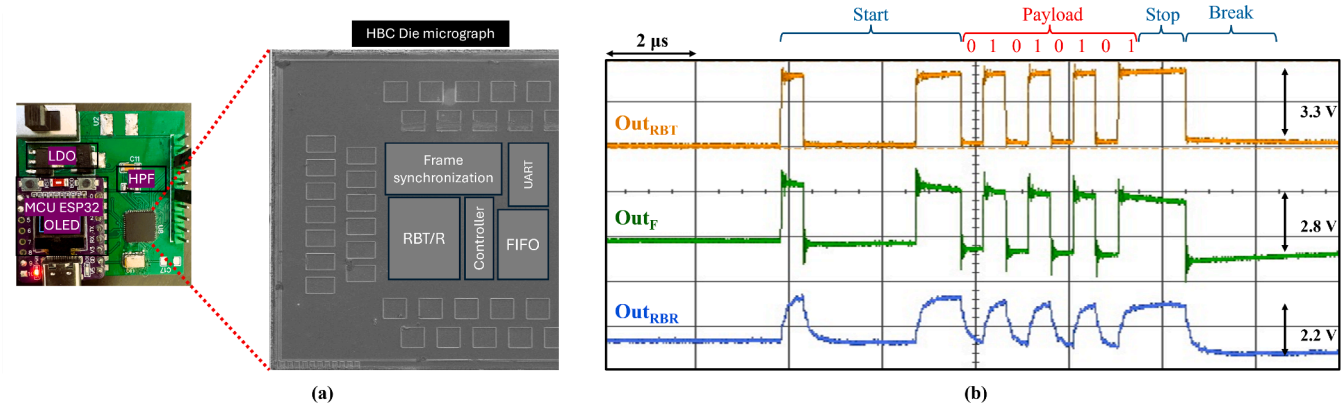

Fig. 4. (a) Die micrograph of the fabricated CG-HBC TRx and the evaluation PCB showing the implementation. (b) Signal outputs from the RBT, HPF, and RBR demonstrating successful digital signal transmission at 2 Mbps data rate.

Algorithm 1 Transmission protocol for link status detection.

```
Electrode interface module select electrodes i, j
Initialize M, K, P
Initialize bitErrors, totalTx, successfulTx, failedTx, noResponseCount to 0
for each iteration do
    Send byte 0xAA from electrode i and receive at electrode j
    if response is received then
        Count bit errors in response
        Increment successfulTx and reset noResponseCount
    else
        Increment noResponseCount and failedTx
    end if
    if noResponseCount reaches K then
        Set Status to "Disconnected" and reset counters
    end if
    if totalTx reaches M then
        if bitErrors = 0 and failedTx = 0 then
            Set Status to "Connected"
        else if bitErrors ≥ 0 and failedTx = 0 then
            Set Status to "Loose"
        else if failedTx ≥ 0 then
            Set Status to "Intermittent"
        end if
        Compute BER as bitErrors / (successfulTx * P)
        Reset counters
    end if
end for
Return Status
```

sampling intervals, enabling real-time contact verification without interfering with biomedical signal acquisition. This multi-rate approach ensures compatibility with standard ECG protocols while adapting to different clinical scenarios.

The pseudocode of the transmission protocol is outlined in Algorithm 1 that assesses the communication link between two generic electrodes. The process begins by selecting two electrodes from multiple available options and then defining two constants, M and K. The constant M represents the number of consecutive transmissions that form an evaluation window for assessing link quality. After every M transmissions, the system determines whether the connection status should be classified as "connected," "loose," or "intermittent," based on the relative success or failure rate of the transmissions within that window. Conversely, the constant K defines the threshold for declaring a complete disconnection, corresponding to the number of consecutive failed transmissions required before the system marks the link as "disconnected." By ensuring K is greater than M, the protocol avoids misclassifying short-term noise disturbances or transient losses as disconnections, thereby improving the robustness of link monitoring. Both parameters can be tuned according to user requirements and application-specific considerations, enabling adaptable performance across diverse electrode configurations or experimental scenarios. Other key variables that include counters for tracking various metrics, such as the total number of transmissions, occurrences of bit errors, and the counts of successful, failed, and no-response transmissions, are also initialized to 0.

The algorithm initiates a transmission loop by sending a predefined byte (`0xAA`) through the body and waits for a response from the Rx. If a response is received, the transmitted and received values are compared to detect bit errors. Any identified errors are logged, and the counters for transmissions and errors are updated. If no response is received, the no-response counter is incremented. If it exceeds a threshold K, the system enters a Disconnected state, signaling a failure in maintaining the communication link. At this point, all counters are reset, and the system prepares for reinitialization to restore connectivity. Following the completion of a specified number of transmissions, the algorithm performs a detailed evaluation of the communication link's quality. It calculates the BER, a critical metric that quantifies the accuracy and reliability of data transmission. It also calculates comprehensive statistics, including transmission counts and error occurrences, providing real-time feedback for system evaluation. Based on the accumulated metrics, the connection is categorized into one of three states: Connected, which indicates error-free and reliable communication; Intermittent, which suggests intermittent transmission failures; or Loose, which denotes occurrences of bit errors despite an otherwise stable connection. The counters are reset after each evaluation phase to prepare the system for subsequent verification cycles. A mapping between BER and transmission failure ranges for each connection state is presented in Table 1. Alert sensitivity for detecting loose or intermittent connections is tunable via BER and failed-transmission thresholds, alongside window parameters M and K. This configurability enables clinicians to balance sensitivity and specificity by application: lower M/K for high-sensitivity clinical monitoring to capture early degradation, and higher M/K for home settings to reduce alert burden while preserving detection of significant failures.

2.3. Electrode contact status detection

Since Algorithm 1 determines the link status between electrode pairs, it is not directly possible to infer the connectivity status of individual electrodes. A missing link suggests that at least one electrode is faulty; however, identifying a specific faulty or disconnected electrode requires at least two fully connected reference electrodes, that is, the links

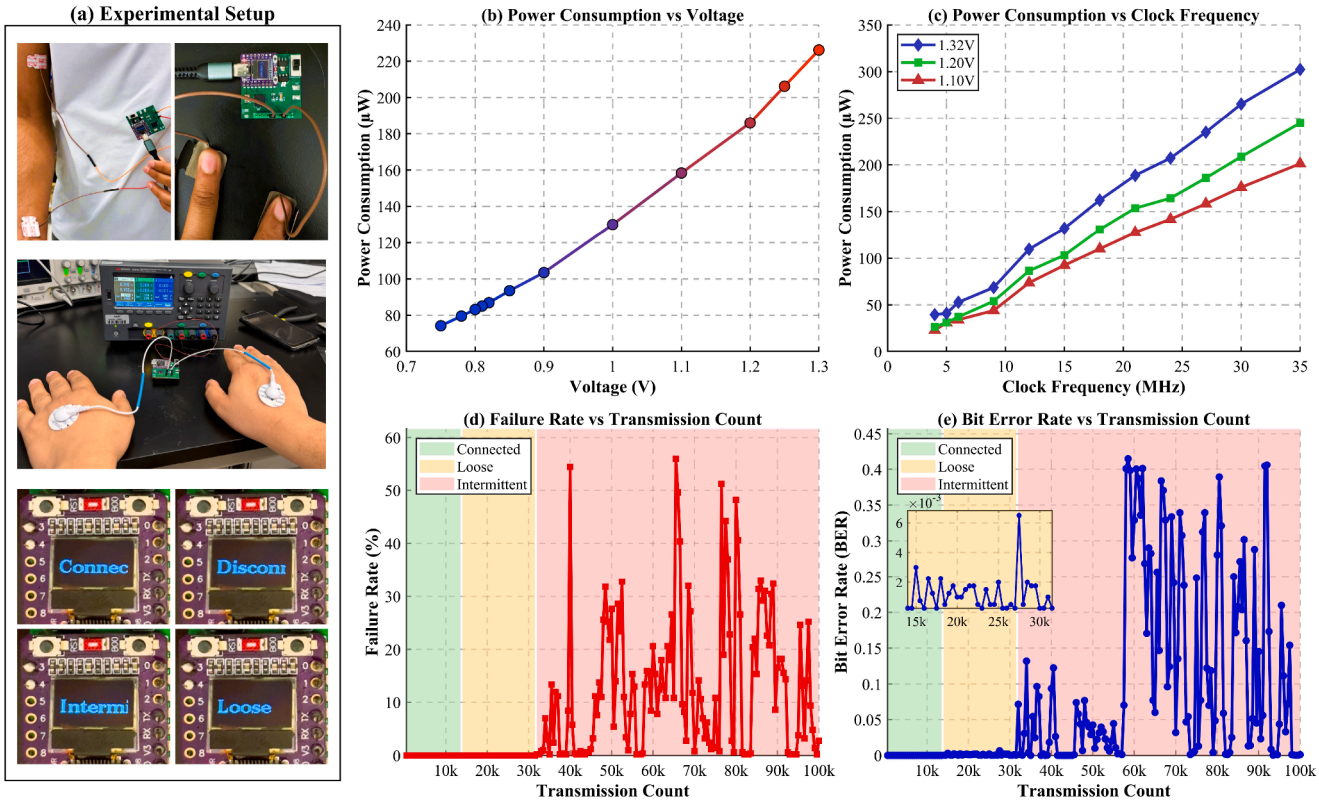

Fig. 5. (a) (a) Electrode placement for signal transmission and power analysis on the human body with OLED display showing real-time connection status. (b) Core power consumption versus supply voltage at 27 MHz, demonstrating linear scaling with minimum operating voltage of 0.78 V. (c) Power consumption at various clock frequencies showing frequency-power correlation. (d) Failed transmission analysis across different contact states. (e) BER analysis showing error-free transmission for connected states, $\approx 10^{-3}$ for loose connections, and higher rates for intermittent contacts.

Table 1
Link status determination based on BER and transmission performance.

Bit Error Rate	Failed Transmission	Evaluation Window	Final State
0	0	M transmissions; $K > M$	Connected
> 0	0	M transmissions; $K > M$	Loose
≥ 0	> 0	M transmissions; $K > M$	Intermittent
–	K consecutive	K transmissions; $K > M$	Disconnected

between these electrodes exhibit no bit errors or transmission failures, allowing each to serve as a reliable reference. Consequently, an exhaustive link status evaluation among N electrodes can identify up to $F_{\max} = \lfloor \frac{N}{2} \rfloor$ faulty electrodes.

To generalize the system, we represent the set of electrodes as an undirected graph $\mathcal{G}(\mathcal{N}, \mathcal{E})$, where $\mathcal{N}$ denotes the set of N electrodes (i.e., vertices) and $\mathcal{E}$ represents the set of $L = \frac{N(N-1)}{2}$ links (i.e., edges), each labeled with their connetion status. Due to the bidirectional nature of communication links, $\mathcal{G}$ is inherently undirected. Constructing $\mathcal{G}(\mathcal{N}, \mathcal{E})$ requires executing Algorithm 1 L times to verify all pairwise connections. Once the graph is constructed, graph traversal algorithms can be employed to determine the connectivity status of all [20], whose worst-case (i.e., having more than $F_{\max}$ disconnected electrodes) computational complexity is $\mathcal{O}(N^2)$.

Since graph traversal operates at the computation level, the total time required for detecting electrode statuses is predominantly dictated by the time needed to construct the graph. Therefore, BCAS system parameters must be carefully tuned based on the application requirements. For instance, in an ECG monitoring scenario, the connectivity status of electrodes must be determined within an ECG cycle, given by $T = \frac{60}{HR}$ s, where HR is the heart rate in beats per minute. Considering that Algorithm 1 requires at most K packet transmissions per link evaluation, the condition $\frac{N(N-1)}{2} K\Delta \leq T$ must hold to ensure graph construction within the ECG interval, where Δ is the packet duration. Accordingly, the maximum allowable packet transmissions per link is given by $K_{\max} = \frac{2T}{N(N-1)\Delta}$. For example, in a 12-lead ECG system with $N = 10$, we obtain $F_{\max} = 5$ and $K_{\max} = \{2020, 1010, 101\}$ for $HR = 60$ bpm and $\Delta = \{11, 22, 220\}\mu$s, respectively. The determined $K_{\max}$ values demonstrate suitability for ECG signal conditions, and the same parameter framework can be readily adapted for other biomedical monitoring applications with appropriate tuning. In the next section, we present a proof-of-concept implementation of the BCAS system, focusing on a single electrode pair, and demonstrate that $K = 50$ is sufficient for reliable link status detection.

3. Hardware implementation and performance analysis

This section provides a comprehensive evaluation of the proposed BCAS. The proposed BCAS is designed as a comprehensive electrode contact monitoring solution, utilizing an ESP32 microcontroller paired with an integrated OLED display and a custom-designed CG-HBC TRx integrated circuit. The CG-HBC TRx is designed and implemented with a focus on optimizing area efficiency, throughput, and power consumption. It is fabricated using TSMC 65-nm CMOS technology, with implementation carried out using Cadence's industry-standard digital design tools. Following the ASIC flow, we first develop system-level models in MATLAB to validate the design concept and determine optimal design parameters. This is followed by RTL implementation in Verilog, with detailed functional verification using Cadence Xcelium to ensure the proper operation of all components. The design then undergoes synthesis using Cadence Genus to create an optimized gate-level implementation. Subsequent physical design stages, including floorplanning, clock tree synthesis, and place-and-route, are executed using Cadence Innovus,

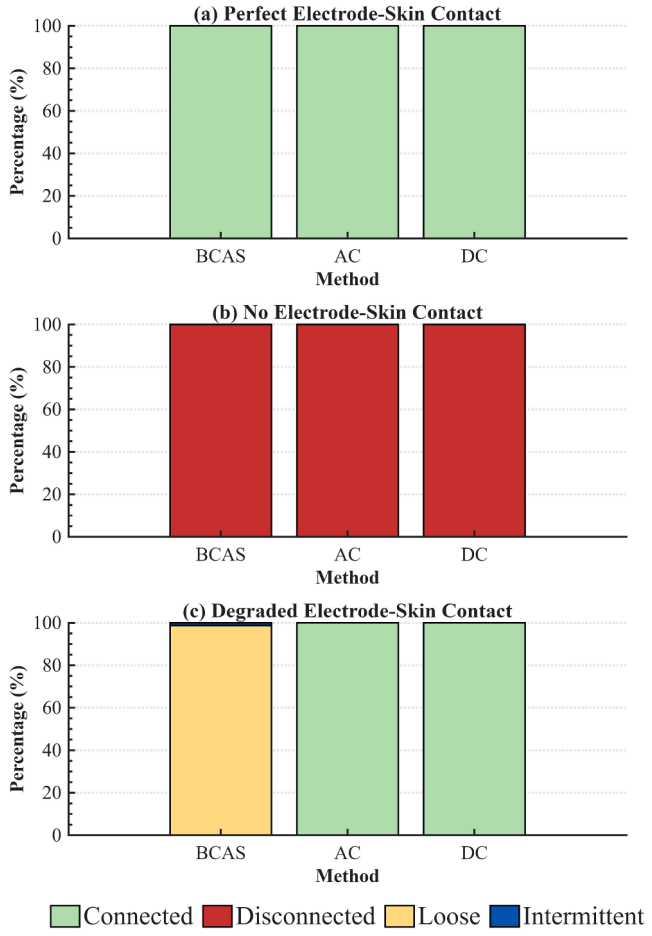

Fig. 6. Electrode connection scenarios for performance evaluation: (a) perfect electrode-skin contact, (b) no electrode-skin contact, and (c) degraded electrode-skin contact.

focusing on layout optimization, resource utilization, and timing constraints. Post-layout verification is performed using Cadence Xcelium with back-annotated SDF files to validate timing performance under realistic conditions. Clock and enable gating techniques are applied across all modules to further enhance power efficiency.

The compact design achieves an area of 0.1 mm^2 while incorporating 18K logic gates. The modular architecture allows easy integration of the CG-HBC TRx as an IP block in future medical ASICs. The die micrograph of the fabricated CG-HBC TRx, along with the evaluation PCB, is shown in Fig. 4(a). Fig. 4(b) presents experimental signal measurements from the BCAS prototype operating with two electrodes at a 2 Mbps data rate. The oscilloscope traces demonstrate the signal propagation through the system, capturing the CG-HBC Tx output (Out_{RBT}), the HPF filtered output (Out_F), and the successfully received signal (Out_{RBR}). These measurements validate the integrity of digital signal transmission through the human body channel and confirm proper system functionality.

Fig. 5(a) illustrates the practical deployment scenario, with electrodes positioned on the human body and the corresponding connection status displayed on the OLED interface. The MCU's integrated OLED display provides real-time visualization of electrode connectivity, significantly enhancing system usability by allowing healthcare professionals to monitor performance and identify issues instantaneously. Using detection parameters of $K = 50$ and $M = 10$, the system successfully demonstrates accurate link status identification based on the computed connectivity metrics. Power consumption characteristics of the proposed CG-HBC are comprehensively evaluated under varying operating conditions. Fig. 5(b) shows the core power consumption measured at a 27 MHz clock frequency while varying the supply voltage from 0.7 V to 1.3 V. The results demonstrate that power consumption scales linearly with supply voltage reduction while maintaining full operational functionality down to the minimum operating voltage of 0.78 V, indicating excellent power scalability for battery-constrained applications. Fig. 5(c) presents power consumption measurements across different operating frequencies corresponding to the supported data rates. As expected, power consumption exhibits a direct correlation with clock frequency and data rate due to increased switching activity. At the process corner with a 1.1 V supply voltage, the proposed CG-HBC TRx achieves optimal power efficiency of approximately 23.10 μW when operating at a 2 Mbps data rate with a 4 MHz clock frequency.

In the subsequent analysis, comprehensive electrode connectivity assessment is conducted through systematic evaluation of bit error rate (BER) and transmission failure metrics across varying contact conditions. The experimental protocol employs $M = 500$ and $K \gg M$ over 100,000 total transmissions to ensure statistical significance and robust performance characterization. During these measurements, intentional arm movements are introduced to emulate realistic operating conditions and induce dynamic variations in electrode contact. Fig. 5(d) presents the failed transmission analysis across three distinct electrode contact states. Under optimal contact conditions and loose connection scenarios, failed transmissions remain at zero, indicating reliable signal propagation through the human body channel. However, intermittent contact conditions exhibit elevated failure rates, providing a clear discriminatory metric for contact quality assessment. The corresponding BER analysis, illustrated in Fig. 5(e), demonstrates the system's sensitivity to contact degradation. Error-free transmission (BER = 0) is consistently achieved under optimal electrode contact, while loose connections exhibit BER values in the 10^{-3} range. Notably, intermittent contact conditions show a strong correlation between increased transmission failures and elevated BER, with error rates rising significantly as contact reliability deteriorates.

The proposed methodology demonstrates robust classification capability, accurately distinguishing between connected, loose, and intermittent electrode states through dual-metric analysis of BER and transmission success patterns. This multi-parameter approach enables error-free contact state identification with high specificity and sensitivity. The classification accuracy is fundamentally dependent on the optimization of detection parameters M and K, which determine the statistical sample size and temporal resolution of the evaluation protocol, highlighting the importance of parameter tuning for specific clinical applications. While the electrode interface module can be implemented using analog multiplexer and demultiplexer circuits [21], this functionality is not included in the current implementation.

4. Comparison of lead-off detection methods

To establish a comprehensive performance benchmark, the proposed BCAS is systematically compared with conventional AC and DC lead-off detection methods. The AC and DC detection schemes are implemented using the ADALM2000 (M2K) mixed-signal processing platform from Analog Devices, incorporating the lead-off detection architecture derived from the AD8233 heart rate monitor IC [11,22]. A consistent experimental protocol is employed across all modalities, maintaining identical electrode placements while acquiring lead-off status data sequentially. Signal processing and statistical evaluation are conducted in MATLAB to ensure standardized data handling and uniform computation of performance metrics. Each detection method is evaluated over multiple consecutive iterations to generate a statistically robust dataset. For BCAS, each iteration employs $M = 10$, and for the disconnected case, $K = 50$, consistent with the initial parameter settings.

The baseline assessment is performed under ideal conditions using new electrodes, as illustrated in Fig. 6(a) and Fig. 6(b). In Fig. 6(a), all electrodes maintain proper contact, while in Fig. 6(b), all electrodes are intentionally disconnected. These two scenarios define the full range

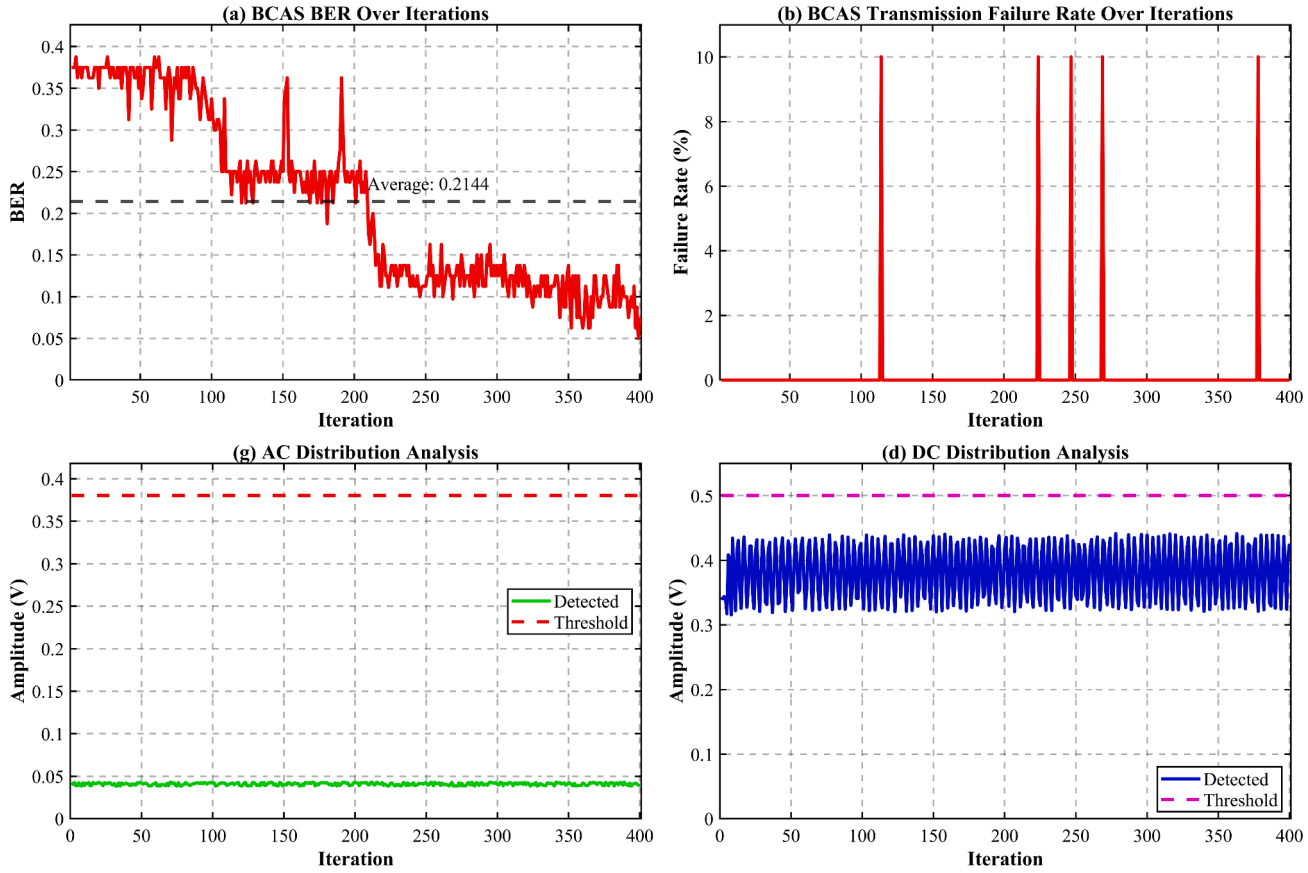

Fig. 7. Comparative evaluation under degraded electrode conditions. (a) BER analysis, (b) transmission failures, (c) AC signal distribution with threshold, and (d) DC signal distribution with threshold.

of connection states and serve as references for evaluating detection accuracy. Under these ideal conditions, BCAS demonstrates detection performance comparable to both AC and DC methods, where the threshold values for these methods are determined based on the specific M2K hardware configuration and the corresponding resistor values used in this experimental setup. For more realistic operating conditions, a challenging test scenario is introduced by replacing one electrode with a deliberately degraded counterpart, mimicking the effects of aging and poor skin contact. This results in varying degrees of performance degradation. As shown in Fig. 6(c), BCAS exhibits enhanced sensitivity in detecting compromised connections under the tested conditions. Within this experimental framework, none of the iterations achieved error-free transmission, with all exhibiting measurable errors that highlight BCAS's ability to identify degraded contact quality. Unlike the DC and AC methods, which classified all iterations as connected within their respective thresholds, BCAS identified more than 98 % of the iterations as loose connections, while the remaining cases are detected as intermittent.

The comparative analysis of BER is presented in Fig. 7(a), while Fig. 7(b) shows the transmission failures observed under these specific degraded conditions. Under the imposed degraded electrode conditions, BCAS demonstrates a notable diagnostic advantage over the conventional methods tested. This outcome suggests BCAS's enhanced diagnostic precision and improved reliability in detecting compromised electrode integrity within this experimental setup. Fig. 7(c) shows the distribution of AC values obtained, indicating that the amplitude falls below the predetermined threshold value consistent with AC lead-off detection principles. Similarly, Fig. 7(d) presents the corresponding DC signal distribution along with the predetermined threshold value specific to the DC detection method. The enhanced capability of BCAS stems from its complete packet analysis approach, in contrast to the threshold-based comparative techniques used in DC and AC methods. While this method introduces additional timing complexity, it enables a more detailed and accurate assessment of connection quality. Despite the increased processing demands, BCAS remains well-suited for biomedical applications–as demonstrated in earlier sections–where robust and precise detection of lead-off events is essential for maintaining signal integrity and ensuring reliable clinical monitoring. A significant advantage of BCAS is that it employs a signal attenuation-based approach, which directly addresses the signal degradation challenges encountered in biomedical measurements.

Table 2
Comparing existing HBC TRx design with the proposed HBC TRx.

Design Parameters	[23]	[24]	[25]	[26]	[27]	This work
CMOS Process (nm)	65	65	90	55	65	65
Communication	FSDT	OOK	FSDT	FSK	AE	RBT
Power Supply (V)	1.2	0.5	1.2	1.2	1.2	1.1
Clock (MHz)	210	0.05-1	42	2	42	4
Data Rate (kbps)	1312.5	1	1312.5	500	5250	2000
Power (μW)	4140	0.415	784	710	85.3	23.10
E_b (pJ/bit)	3155	415	598	1420	16	11.55

5. Discussion and future scope

The hardware implementation and comparative analysis of various lead-off detection methods highlight the potential of the proposed system. In the experiments, commercially available wet electrodes are used. The skin surface is cleaned with a wet tissue before electrode placement to ensure good contact and reduce impedance variability. This procedure is applied consistently across all measurements to

maintain experimental reliability. This study further benchmarks the proposed HBC TRxs against existing literature, evaluating communication methods based on autoencoder (AE), frequency-shift keying (FSK), on-off keying (OOK), and frequency-selective digital transmission (FSDT). Table 2 demonstrates that the proposed approach achieves superior energy efficiency while maintaining data rates comparable to prior implementations. This performance improvement primarily results from the elimination of analog front-end requirements inherent to conventional designs.

Despite these promising results, the study has some limitations. A major experimental constraint arises from the sequential application of the three detection schemes (AC, DC, and BCAS) rather than their concurrent execution. In practice, it is not feasible to transmit and receive three types of signals simultaneously between the same electrode pair. Consequently, slight variations in electrode contact conditions between successive measurements introduce variability in the results. This temporal factor inherently adds a degree of uncertainty to the comparative analysis and represents a fundamental limitation of the evaluation methodology. To minimize temporal errors, the measurements are conducted sequentially with only a few seconds of delay between each mode. Another limitation of this study is that the system is tested using intentionally degraded electrodes to emulate real-world conditions. However, practical testing in an actual environment using real biomedical signal measurements is not yet performed. Furthermore, the prototype implementation is currently limited to a single electrode pair. The electrode interface module is implemented manually with only a pair of electrodes, but automation can be incorporated in future versions using dedicated hardware components.

The current experimental measurements are performed under controlled humidity conditions, and the effects of humidity or sweating are not analyzed in this study. Degradation of the skin-electrode contact due to these factors may lead to loose or intermittent connections, which remains beyond the present scope. Future work focuses on developing an integrated System-on-Chip solution that combines the HBC TRx with a reconfigurable electrode interface module and a dedicated processing unit for analysis under different environmental conditions. This integrated approach enables comprehensive multi-electrode monitoring while achieving a reduced form factor and lower power consumption. It enhances the reliability and autonomy of healthcare systems by automatically identifying electrode connection states and generating warning signals for faulty connections, thereby minimizing the need for manual inspection.

6. Conclusion

This paper presents a novel BioContact Assurance System leveraging common-ground human body communication for real-time electrode contact monitoring. The system employs direct digital transmission through the human body, eliminating complex analog front-end circuitry while achieving better performance compared to conventional DC and AC lead-off detection methods. The custom-designed integrated circuit, fabricated in TSMC 65 nm technology, achieves exceptional energy efficiency of 11.55 pJ/bit and power consumption of only 23.10 μW in a compact 0.1 mm^2 footprint. The system successfully classifies electrode states as connected, loose, intermittent, or disconnected through dual-metric analysis of bit error rates and transmission patterns. The modular architecture enables seamless integration into existing biomedical systems without hardware modifications. Future work will focus on developing an integrated System-on-Chip solution combining the HBC TRx with reconfigurable electrode interface module, enabling comprehensive multi-electrode monitoring with reduced form factor and power consumption. The proposed BCAS establishes a new benchmark for electrode contact monitoring, offering enhanced reliability and precision essential for critical healthcare applications.

Data availability

Data will be made available on request.

CRediT authorship contribution statement

Rajat Kumar: Writing – review & editing, Writing – original draft, Visualization, Validation, Software, Methodology, Investigation, Formal analysis, Data curation, Conceptualization; **Abdelhay Ali:** Writing – review & editing, Visualization, Validation, Supervision, Methodology, Formal analysis, Data curation; **Abdulkadir Celik:** Writing – review & editing, Visualization, Validation, Supervision; **Ahmed M. Eltawil:** Writing – review & editing, Visualization, Validation, Supervision, Resources, Project administration, Funding acquisition.

Declaration of competing interest

The authors declare that they have no known competing financial interests or personal relationships that could have appeared to influence the work reported in this paper, other than the funding sources disclosed in the Acknowledgments section.

Acknowledgments

The research reported in this publication was partially supported by funding from KAUST Center of Excellence for Smart Health, under award number #5932 and NEOM under award number #4819. The experiments were conducted with the approval of the Institutional Biosafety and Bioethics Committee (IBEC) under the reference number 20IBEC30.

References

[1] A. Celik, K.N. Salama, A.M. Eltawil, The internet of bodies: a systematic survey on propagation characterization and channel modeling, IEEE Internet Things J. 9 (1) (2021) 321–345.
[2] A. Ali, A.N. Abdelrahman, A. Celik, A.M. Eltawil, EQS-band human body communication through frequency hopping and MCU-based transmitter, Smart Health 32 (2024) 100471.
[3] A. Celik, A.M. Eltawil, The internet of bodies: the human body as an efficient and secure wireless channel, IEEE Internet Things Mag. 5 (3) (2022) 114–120. https://doi.org/10.1109/IOTM.001.2100209
[4] Q. Liu, L. Yang, Z. Zhang, H. Yang, Y. Zhang, J. Wu, The feature, performance, and prospect of advanced electrodes for electroencephalogram, Biosensors 13 (1) (2023) 101.
[5] J. Heikenfeld, A. Jajack, J. Rogers, P. Gutruf, L. Tian, T. Pan, R. Li, M. Khine, J. Kim, J. Wang, Wearable sensors: modalities, challenges, and prospects, Lab Chip 18 (2) (2018) 217–248.
[6] Y. Fu, J. Zhao, Y. Dong, X. Wang, Dry electrodes for human bioelectrical signal monitoring, Sensors 20 (13) (2020) 3651.
[7] Y. Wang, F. Miao, Q. An, Z. Liu, C. Chen, Y. Li, Wearable multimodal vital sign monitoring sensor with fully integrated analog front end, IEEE Sens. J. 22 (13) (2022) 13462–13471.
[8] Y. Tang, X. Gu, R. Wu, J. Ding, L. Zhang, F. Yan, H. Ma, X. Bu, A lead-off detection design for an improved front of bioelectrical signal acquisition, in: 2018 IEEE SENSORS, IEEE, 2018, pp. 1–4.
[9] H. Kim, M. Kim, K. Lee, S. Cho, C.S. Park, S. Song, D.S. Keum, D.P. Jang, J.J. Kim, 32.1 A behind-the-ear patch-type mental healthcare integrated interface with 275-fold input impedance boosting and adaptive multimodal compensation capabilities, in: 2023 IEEE International Solid-State Circuits Conference (ISSCC), IEEE, 2023, pp. 1–3.
[10] N. Van Helleputte, M. Konijnenburg, J. Pettine, D.-W. Jee, H. Kim, A. Morgado, R. Van Wegberg, T. Torfs, R. Mohan, A. Breeschoten, et al., A 345 μW multi-sensor biomedical SoC with bio-impedance, 3-channel ECG, motion artifact reduction, and integrated DSP, IEEE J. Solid-State Circuits 50 (1) (2014) 230–244.
[11] A. Devices, AD8233: 50 μA, 2mm × 1.7 mm WLCSP, low noise, heart rate monitor for wearable products, Datasheet, Rev. D, https://www.analog.com/media/en/technical-documentation/data-sheets/ad8233.pdf (2019).
[12] M.R. Baidillah, R. Riyanto, P. Busono, S. Karim, R. Febryarto, A. Astasari, D. Sangaji, W.P. Taruno, Electrical impedance spectroscopy for skin layer assessment: a scoping review of electrode design, measurement methods, and post-processing techniques, Measurement 226 (2024) 114111. https://doi.org/10.1016/j.measurement.2023.114111
[13] K. Polachan, B. Chatterjee, S. Weigand, S. Shreyas, Human body–electrode interfaces for wide-frequency sensing and communication: a review, Nanomaterials 11 (8) (2021) 2152.

[14] E. Alonso, R. Giannetti, C. Rodríguez-Morcillo, J. Matanza, J.D. Muñoz-Frías, A novel passive method for the assessment of skin-electrode contact impedance in intraoperative neurophysiological monitoring systems, Sci. Rep. 10 (1) (2020) 2819.
[15] R. Manzo, A. Apicella, P. Arpaia, F. Caputo, a. Nicola Moccaldi, Real-time detection of skin-electrode adhesion based on embedded neural networks for bioimpedance spectroscopy, IEEE Access 13 (2025) 155385–155398. https://doi.org/10.1109/ACCESS.2025.3605928
[16] M. Li, Y. Song, Y. Hou, N. Li, Y. Jiang, M. Sulaman, Q. Hao, Comparable investigation of characteristics for implant intra-body communication based on galvanic and capacitive coupling, IEEE Trans. Biomed. Circuits Syst. 13 (6) (2019) 1747–1758. https://doi.org/10.1109/TBCAS.2019.2940827
[17] M.D. Pereira, G.A. Alvarez-Botero, F.R. de Sousa, Characterization and modeling of the capacitive HBC channel, IEEE Trans. Instrum. Meas. 64 (10) (2015) 2626–2635.
[18] J.F. Zhao, X.M. Chen, B.D. Liang, Q.X. Chen, A review on human body communication: signal propagation model, communication performance, and experimental issues, Wireless Commun. Mobile Comput. 2017 (1) (2017) 5842310.
[19] G.A. Alvarez-Botero, Y.K. Hernandez-Gomez, C.E. Tellez, J.F. Coronel, Human body communication: channel characterization issues, IEEE Instrum. Meas. Mag. 22 (5) (2019) 48–53.
[20] N. Christofides, The optimum traversal of a graph, Omega 1 (6) (1973) 719–732.
[21] T. Instruments, CD74HCx4067 high-speed CMOS logic 16-channel analog multiplexer and demultiplexer, Datasheet, Rev. D https://www.ti.com/lit/ds/symlink/cd74hc4067.pdf (2024).
[22] A. Devices, ADALM2000 advanced active learning module, Eval. Board, USB-powered software-defined instrument https://www.analog.com/en/resources/evaluation-hardware-and-software/evaluation-boards-kits/adalm2000.html (2024).
[23] B. Zhao, Y. Lian, A.M. Niknejad, C.H. Heng, A low-power compact IEEE 802.15. 6 compatible human body communication transceiver with digital sigma–delta IIR mask shaping, IEEE J. Solid-State Circuits 54 (2) (2018) 346–357.
[24] S. Maity, N. Modak, D. Yang, M. Nath, S. Avlani, D. Das, J. Danial, P. Mehrotra, S. Shreyas, Sub-μWRComm: 415-nW 1–10-kb/s physically and mathematically secure electro-quasi-static HBC node for authentication and medical applications, IEEE J. Solid-State Circuits 56 (3) (2021) 788–802.
[25] A. Ali, S.M. Ahmed, M.S. Sayed, A. Shalaby, Deep learning-based human body communication baseband transceiver for WBAN IEEE 802.15. 6, Eng. Appl. Artif. Intell. 115 (2022) 105169.
[26] G. Gu, C. Yang, J. Zhao, S. Du, Y. Luo, B. Zhao, A 2m-range 711μW body channel communication transceiver featuring dynamically-sampling bias-free interface front end, IEEE Trans. Biomed. Circuits Syst. PP (2024) 1–12. https://doi.org/10.1109/TBCAS.2024.3439619
[27] A. Ali, A.N. Abdelrahman, A. Celik, M.E. Fouda, A.M. Eltawil, A robust auto-encoder HBC transceiver with CGAN-based channel modeling, IEEE Sens. J. 25 (9) (2025) 15935–15949.